ARMY RESEARCH LABORATORY

Crack Stability and Its Effect on Single-Edge-Precracked Beam (SEPB) Fracture Toughness of Hot-Pressed Silicon Nitride Beam Specimens

by Isa Bar-On, Francis I. Baratta,
and Kyu Cho

ARL-TR-1407

June 1997

The findings in this report are not to be construed as an official Department of the Army position unless so designated by other authorized documents.

Citation of manufacturer's or trade names does not constitute an official endorsement or approval of the use thereof.

Destroy this report when it is no longer need. Do not return it to the originator.

Army Research Laboratory
Aberdeen Proving Ground, MD 21005-5069

ARL-TR-1407 **June 1997**

Crack Stability and Its Effect on Single-Edge-Precracked Beam (SEPB) Fracture Toughness of Hot-Pressed Silicon Nitride Beam Specimens

Isa Bar-On
Worcester Polytechnic Institute

Francis I. Baratta, Kyu Cho
Weapons and Materials Research Directorate, ARL

Abstract

The effect of stable crack extension on fracture toughness test results was determined using single-edge-precracked- beam specimens. Crack growth stability was examined theoretically for bars loaded in three-point bending under displacement control. The calculations took into account the stiffness of both the specimen and the loading system. The results indicated that the stiffness of the testing system played a major role in crack growth stability. Accordingly, a test system and specimen dimensions were selected which would result in unstable or stable crack extension during the fracture toughness test depending on the exact test conditions. Hot-pressed silicon nitride bend bars (NC132) were prepared with precracks of different lengths resulting in specimens with different stiffnesses. The specimens with the shorter precracks and thus higher stiffness broke without stable crack extension, while those with long cracks, and lower stiffness broke after some stable crack extension. The fracture toughness values from the unstable tests were 10% higher than those from the stable tests. This difference, albeit small, is systematic and is not considered to be due to material or specimen-to-specimen variation. It is concluded that instability due to the stiffness of the test system and specimen must be minimized to ensure some stable crack extension in a fracture toughness test of brittle materials in order to avoid inflated fracture toughness values.

Acknowledgments

The authors wish to thank Mr. Brian Pothier, U.S. Army Research Laboratory (ARL), Aberdeen Proving Ground (APG), MD, and Dr. David Jablonski, Instron, Canton, MA, for their assistance with the mechanical testing. ARL's support of this work is gratefully acknowledged. Part of this work was performed while one of us was a National Research Council Fellow at NASA LeRC, Cleveland, OH.

INTENTIONALLY LEFT BLANK.

Table of Contents

INTENTIONALLY LEFT BLANK.

List of Figures

INTENTIONALLY LEFT BLANK.

List of Tables

INTENTIONALLY LEFT BLANK.

1. Introduction

Stable crack extension is difficult to obtain for very brittle materials in many of the loading geometries for which the crack extends into an increasing K-field. For ceramic materials with flat R-curves, stability is all but unattainable when conventional test conditions are used. Nevertheless, it appears that stable crack extension would be desirable and even necessary for fracture experiments that need to be well controlled, such as fracture toughness, R-curve, or fatigue crack growth measurements. The implicit question here is whether these quantities are defined (or used) for a stably propagating crack or for the onset of crack extension in an unstable manner. The answer to this question would be significant if the results obtained from tests with stable crack extension differ from those obtained when only the onset of unstable fracture is experienced.

Previous work to be subsequently discussed indicates that unstable fracture tends to inflate the fracture toughness value when compared to the value obtained for stable crack extension. Thus, the attainment of stable crack growth during fracture is not only worthwhile pursuing but indeed may be necessary to the performance of a valid fracture toughness test.

Germane to the subject of stable crack growth and fracture of brittle materials is a discussion on the definition of fracture toughness. In his review of fracture mechanics techniques as applied to brittle materials, Freiman [1] made specific reference to the definition of fracture toughness (K_{IC}) as defined by ASTM Committee E24 [2] as: ". . . the crack-extension resistance under conditions of crack-tip plane strain." Freiman [1] further states: "For example, in mode I *for slow rates of loading** and negligible plastic-zone adjustment, plane-strain fracture toughness is the value of stress-intensity factor designated K_{IC} [$FL^{-3/2}$] as measured using the operational procedure specified in Test Method E399 [3], that provides for the measurement of crack-extension resistance *at the start of crack extension* and provides operational definitions of crack-tip sharpness, start of crack extension, and crack-tip plane strain." Freiman [1] further commented that "This is clearly not what most of us mean by critical fracture toughness of ceramics." A footnote was suggested (but not accepted by

* Italics are added by the present authors.

the ASTM E24 Committee) to be added to Test Method E399, which would allow using the symbol K_{IC} to designate plane-strain fracture toughness at the onset *of rapid crack extension* under conditions specified by the method.

The opposing views between those concerned with fracture toughness of metallic materials and those having similar concerns in ceramic materials could not have been better underscored. The fracture mechanics specialist experienced in testing metals thinks in terms of an intrinsic fracture toughness for each material, usually determined at the start of quasi-static crack extension [4]; whereas the ceramist believes that rapid crack extension is a necessary requirement when testing ceramic materials mostly in order to avoid well-recognized environmental effects. On the other hand, fracture mechanists have determined [5] that if stress intensity loading rates for metallic materials are kept in the quasi-static regime, specifically between 0.55 and 2.75 MPa$\sqrt{m}$/s, and if the material can be considered linearly elastic, in spite of some plasticity at the crack tip, then neither environmental nor dynamic effects will prevail. Fortunately, plasticity aids in ensuring stable crack growth during fracture of metallic materials, and thus, quasi-static crack extension is realized during fracture. Unfortunately, the ceramist does not experience this luxury when attempting to determine mechanical properties of many brittle materials.

Further complications are encountered during testing when ceramics are environmentally sensitive (see, for example, Weiderhorn [6]). In addition, such materials can be strain-rate sensitive, i.e., the dynamic to quasi-static fracture initiation toughness ratio can be greater than 1.0 (see, for example, Suresh et al. [7]). Unless this information is known or determined, a priori fracture toughness test results will have no base of reference.*

There have been a spate of papers in the literature concerning the subject of stable fracture of quasi-brittle and brittle materials. A few of these papers that are pertinent to the present work are discussed in the following paragraphs by way of further introduction.

---

* It would appear that an appropriate base of reference for mechanical property tests of brittle materials would be testing at quasi-static crack extension, if possible, in a nonhostile environment for those materials that are suspected of being susceptible to both dynamic loading and to the environment.

Nakayama [8] was able to obtain stable and semistable crack growth during fracture of glass and firebrick beams. He experimentally showed that the effective fracture energy was valid only for perfectly stable fractures. In fact, Nakayama's effective fracture energy data, if related to the fracture toughness parameter (K_C), indicates an increase of greater than 40% for a semistable fracture, as compared to that of stable fracture. His major conclusion was that, in order to successfully measure fracture energy of brittle beam specimens, one must have stable crack growth and this can be realized using a stiff testing system.

Several papers, e.g., Clausing [9], Bluhm [10], and Schimoeller [11], have provided theoretical crack stability analyses applied to linear elastic systems, all based on similar principles. Clausing [9] determined the compliance of beam and compact specimens theoretically. He used these formulations in stability criteria for these specimens.

Bluhm [10] provided stability formulations for bend specimens having a chevron notch (CV) or a straight-through crack (STC). He was motivated by an alternative approach to instability using the "work-of-fracture" (WOF) specimen proposed by Tattersall and Tappin [12]. He was able to provide such stability criteria for the three-dimensional (3-D) CV and WOF specimens because of a previous paper intended for that purpose [13]. In this latter paper, an approximate "slice synthesis" technique aided in analytically describing the compliance.

A displacement-controlled closed-loop testing system was considered by Schimoeller [11]. Stability enhancement was predicted for the improved system response due to the addition of closed-loop considerations. However, Schimmoeller claims that the four-point bend specimen is always unstable, which contradicts several authors, including Clausing [9] and Bluhm [10].

All three of these authors [9–11] realized the important role of the testing system compliance or stiffness in attaining stability during fracture. Also, it was noted by Clausing [9] and Bluhm [10] that under no circumstances would a load-controlled STC beam system display stable crack growth.

Cooper's [14] study of rock materials using three-point bend specimens agree with Nakayama [8]. Cooper [14] understood the importance of the loading system stiffness and in attaining stable crack growth, as well as providing a suitable starter notch.

Mai and Atkins [15] provided a compendium of stability factors for many test piece geometries under different loading conditions, such as load and crosshead-displacement controlled and comparisons with experimental results. They supplement these results with experimental methods of promoting crack stability for inherently unstable situations.

Recently, Baratta and Dunlay [16], using Bluhm's analysis, focused on the STC four-point and three-point bend specimens under displacement-controlled loading. Even though they used the idealized criteria, they were able to experimentally predict the crack length at which stability occurred for a quasi-brittle material such as polymethylmethacrylate (PMMA). They showed that the three-point loaded beam had greater stability potential than the four-point loaded beam. Further, it was noted that the onset of stable fracture yielded increasingly lower values of K_{Ic}. This trend was also observed by Underwood et al. [17] in the fracture testing of standard ASTM E399 center loaded bend bars of tungsten, a brittle metallic material.

Sigl [18] recently advanced the theoretical analyses mentioned previously, where stability criterion of an "everyday" testing situation were explored. This author examined the stability of three-point flexure STC and CV specimens under constant-load and constant-displacement rate loading of the testing machine, taking into account the load cell compliance, in a closed-loop testing arrangement under constant deflect. This latter situation enhances stability in beam flexure systems, which was also reported in Schimoeller [11].

Recent progress has been made in introducing controlled cracks in ceramic beam specimens such that the difficulties described by Nakayama [6] and Bluhm [10] have been greatly mitigated. Nose and Fujii [19] have reported fracture toughness tests on precracked single-edge beams. The precrack is introduced using the "bridge indentation" method [19]. In this technique, the specimen is initially flawed by microindentation and then compressed between two anvils, one of which is bridged, thus

creating a short pop-in crack. Bar-On et al. [20], as well as Choi, Chulya, and Salem [21], used this technique to evaluate the effect of the precracking parameters on crack emplacement of beam specimens of various ceramics including hot-pressed silicon nitride (HPSN), which was also the material used in this study. The bridge indentation method (or double anvil geometry) was also employed in the present work to initiate precracks of desired length to explore the effect of crack growth stability (or lack thereof) on fracture toughness of brittle materials.

As previously mentioned, the recent work of Baratta and Dunlay [16], and Underwood, Baratta, and Zalinka [17], has shown that unstable crack extension resulted in an apparent increase in fracture toughness compared to that determined during stable crack growth of a quasi-brittle material, PMMA, and tungsten, a more brittle metallic material. In both cases, the transition from stable to unstable behavior was predicted based on a stability analysis. The objective of this work is to show that such an effect persists for a high-performance ceramic material not susceptible to environmentally assisted cracking but sensitive to unstable fracture during testing.

2. Stability Analysis

Previous work by Baratta and Dunlay [16] demonstrated that the three-point loaded beam was generally more stable than the constant moment beam, and thus, this configuration, shown in Figure 1, is examined here. The ASTM E399 Test Method also uses the three-point loaded beam (Annex A.3) as one of several standard fracture test specimens. This test method has been well-established for metallic materials, and it is explored here to see if it has potential as a vehicle to test brittle materials.

Stability considerations are well presented elsewhere [9–11, 18], and thus a general derivation is not repeated here. However, some comments are appropriate: The general stability equation that is used here, taken from Bluhm [10], presumes that an idealized testing system is used when determining fracture toughness of a brittle material. It is inferred that constant crosshead displacement is employed and that rigid body motion occurs between the crosshead of the testing

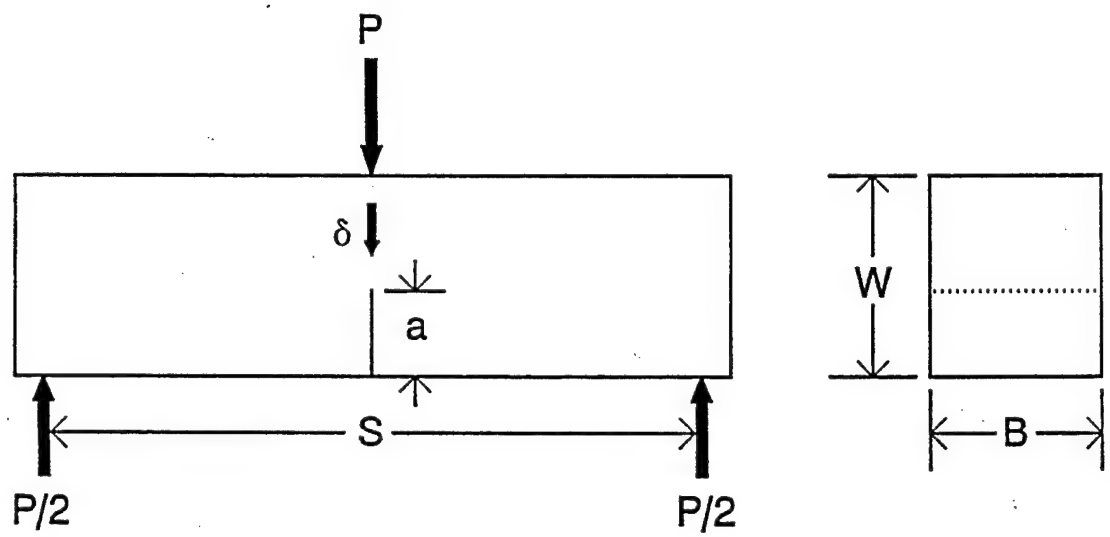

Figure 1. Schematic of Three-Point Load Geometry.

machine and the point of load application to the specimen, i.e., the deflection of the load cell is ignored.

In actual practice, most experimenters, including the present authors, choose "stroke control" when using a closed-loop hydraulic testing machine. Such a testing machine is designed so that a displacement transducer senses the displacement of the actuator, which is then fed back into the hydraulics of the system in a closed-loop arrangement. This signal is, in turn, programmed such that the deflection rate of the specimen is approximately constant. The word "approximately" is used because the deflection rate of the specimen is dependent upon where the sensor is located on the specimen, or with regard to it, and upon the response speed of the system, etc.

Sigl's analysis [18] comes closest to defining the actual test setup described previously. Nevertheless, in order to apply his formulation, additional measurements beyond the usual monitoring of load and displacement would have to be made during testing. Thus Bluhm's analysis [10] was chosen to guide the experiments that are later described. Only the stability formulation under constant crosshead displacement or stroke rate of the testing machine is considered here. The applicable equation is

$$\bar{S} = d^2 (\delta_s/P)/dA^2 - (2/\delta_t/P)\, (d(\delta_s/P)/dA)^2 \leq 0. \qquad (1)$$

Note that the previous stability equation applies to those materials exhibiting flat R-curve behavior. Thus, $\bar{S}$, the stability parameter, is equal to or less than zero. Also, A is the crack area, δ_s/P is the specimen compliance, and δ_t/P is the total compliance, which includes the specimen, the machine compliance, and the fixtures.

If the beam is rectangular in cross-section, then the stability equation for this specific case is simplified to:

$$\bar{S} = d^2\lambda_s/d\alpha^2 - (2/\lambda_t)\,(d\lambda_s/d\alpha)^2 \le 0, \tag{2}$$

where λ_s and λ_t are the normalized compliances, i.e., $\lambda_s = (\delta_s/P)\,EB$, $\lambda_t = \lambda_s + \lambda_m$, $\lambda_m = (\delta_m/P)\,EB$, α is the normalized crack length a/W, where a is the crack length and W is the beam height, E is the modulus of elasticity of the material, and B is the beam width.

When $\bar{S}$ becomes negative, the crack growth during fracture tends toward stability. Note that all that is required in equation 2 is the knowledge of the compliance of both the specimen (as a function of α) and the testing machine, including the fixtures. The compliance of the testing machine and fixturing is usually obtained by experimental means, and the compliance of the specimen can be determined by theoretical considerations (see Baratta [22] and Baratta and Underwood [23]).

The nondimensional plane-strain* compliance of the cracked three-point loaded beam, shown in Figure 1, is considered and derived in Appendix A, which is:

$$\lambda_s = 2\,(S/2W)^2\,\{S/2W + [2.85/(S/2W) - 0.42/(S/2W)^2]/4 + 9(1-\nu^2)\int_0^{\alpha} \alpha[f(\alpha)]^2\,d\alpha\}, \qquad 0 \le \alpha \le 0.70\,. \tag{3}$$

* It was realized that the displacement attributed to the cracked portion of the beam is due to a plane-strain condition rather than plane stress, and for that reason, the quantity $(1-\nu^2)$ is included in both the expressions for the compliance and stability. Note, only a plane stress condition was considered in Baratta and Dunlay [16].

Where S is the beam support length, ν is Poisson's ratio equal to 0.27 for the ceramic material tested here, and [f (α)] is the polynomial expression for the three-point loaded beam incorporated in the following stress intensity factor relationship:

$$K_I = (6Ma^{1/2}/BW^2)\,[f(\alpha)], \tag{4}$$

where M is the applied moment.

A convenient span ratio used in the experimental tests was S/W = 5, resulting in a sixth order polynomial equation as follows:

$$[f(\alpha)] = 1.9228 - 4.1021\alpha + 39.0065\alpha^2 - 191.5842\alpha^3 + 520.5576\alpha^4 - 673.0714\alpha^5 + 343.0783\alpha^6, \qquad 0 \le \alpha \le 0.80\,. \tag{5}$$

The coefficients in equation 5 were obtained by matching the numerical data of Freese [24] (who claims an accuracy of better than 0.5%). These data were obtained by accounting for the effect of contact stress due to the applied load on the stress intensity factor associated with the centrally loaded beam. Thus, equations 4 and 5 are adopted for use here.

For completeness and future use, wide-range stress intensity factor expressions for three-point loaded beams having beam span ratios (S/W) of 4, 5, 6, 7, 8, and 10, as well as the constant moment beam, were determined from the data of Freese [24]. These expressions and the polynomial coefficients are summarized in Appendix B. Although these formulas yield greater accuracy over a wider range of application than equations 4 and 5, they were inconvenient to use in the integration portion of equation 3, and for that reason, equations 4 and 5 were employed.

The stability of the subject beam was determined by taking the first and second derivatives of the compliance, equation 3, and substituting these quantities into equation 2. Normalizing by

$$\Phi = 18\,(1 - \nu^2)\,(S/2W)^2\,\alpha\,[f(\alpha)]^2\,,$$

gives the following nondimensional stability equation defined by $\hat{S} = \bar{S}/\Phi$ for the three-point loaded beam:

$$\hat{S} = \frac{2\,[f(\alpha)]}{[f(\alpha)]} + 1/\alpha - \frac{36\,(1-\nu^2)\,(S/2W)^2\,\alpha\,[f(\alpha)]^2}{\lambda_t}, \quad 0 \le \alpha \le 0.70. \qquad (6)$$

Machine compliance is an important consideration in the design of a stable specimen test system when attempting to determine stability of brittle materials. Clausing [9] indicates that ". . . the compliance of 1.5 is typical of a very stiff loading system, such as a bolt that directly opens the crack. The compliance of 600 is typical of a rather flexible grip system in a tension testing machine." Equation 6 was computer programmed so that the effect of machine compliance from 0 to 600 on stability could be examined for $S/W = 5$ and $0 \le \alpha \le 0.70$. These results are presented in Figure 2; they show the stability parameter $\hat{S}$ for the three-point loaded beam having a span ratio of 5, as a function of crack length ratio α and nondimensional machine compliance λ_m. The reader is reminded that the more negative $\hat{S}$ becomes, the greater the possibility that stability occurs. Therefore, as expected, when λ_m is increased, $\hat{S}$ becomes more positive and thus less stable, as shown in Figure 2.

The threshold of stability, $\alpha_0 = a_0/W$, defined by $\hat{S} = 0$ was determined as a function of λ_m for a span ratio of 5 and is shown in Figure 3. Again, as λ_m is increased, stability tends to decrease; this is reflected in the increase in α_0. This curve, which allows ready prediction of α_0 as a function of machine compliance for the three-point loaded beam having a span ratio of 5, was used to provide guidance to the experimental program described in the experimental procedure section. The discontinuous lines mark the approximate conditions of our experiment.

Polynomial equations of the same form as equation 5 were generated from the data of Freese [24] for span-to-width ratios ranging from 4 to 10. This allowed the specimen compliance to be determined from equation 3 as previously described. These results were, in turn, programmed into

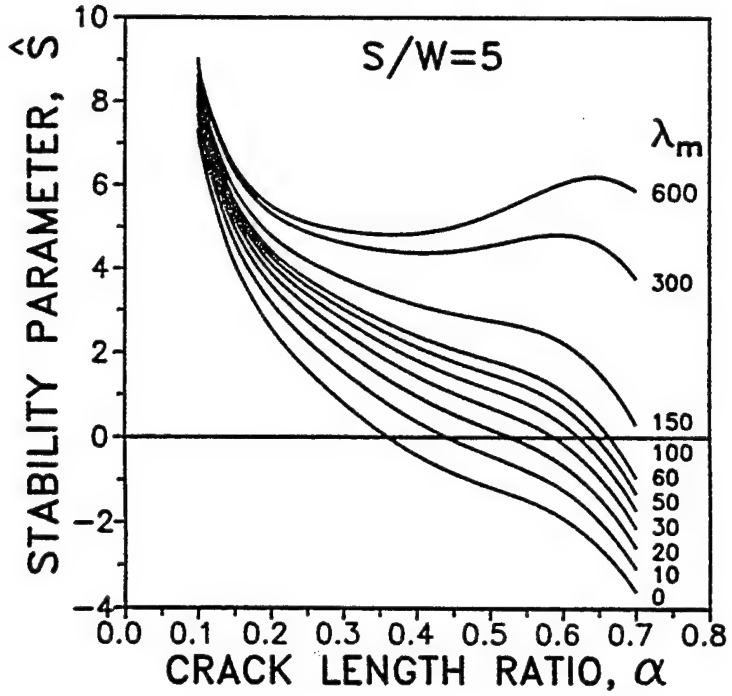

Figure 2. Stability Parameter for the Three-Point Loaded Beam Having a Span-to-Width Ratio of 5, as a Function of Crack Length Ratio, α, for Dimensionless Machine Compliance Values Ranging From 0 to 600.

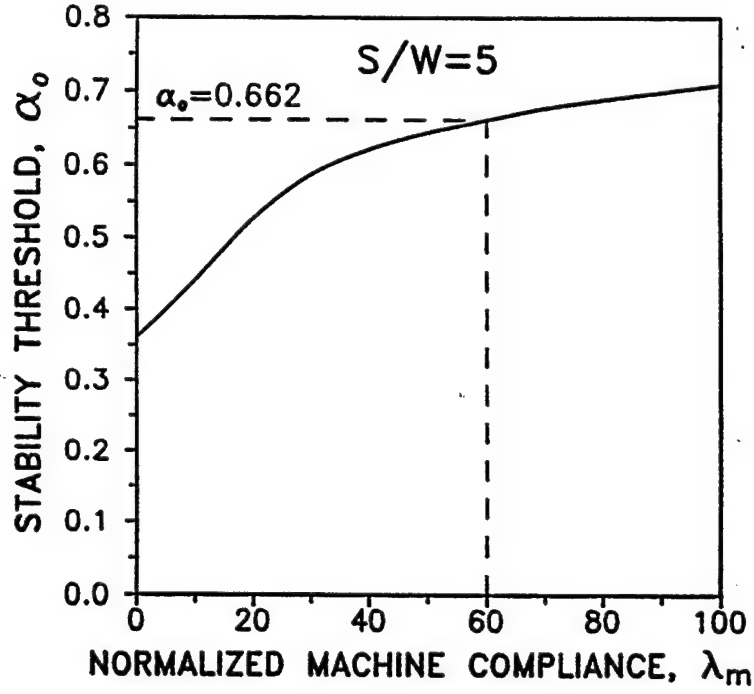

Figure 3. Stability Threshold Crack Length, α_o, for Normalized Machine Compliance Values Ranging From 0 to 600 for the Three-Point Loaded Geometry Having a Span-to-Width Ratio of 5.

equation 6 to obtain the stability parameter, $\hat{S}$, as a function of both beam span ratios and machine compliances. Again, by forcing $\hat{S}$ to be zero, the stability threshold α_0 was obtained. The resulting family of curves is shown in Figure 4 to provide guidance for *stable* fracture toughness testing of brittle materials. Appropriate comments on this subject will be presented in the results and discussion section of this report.

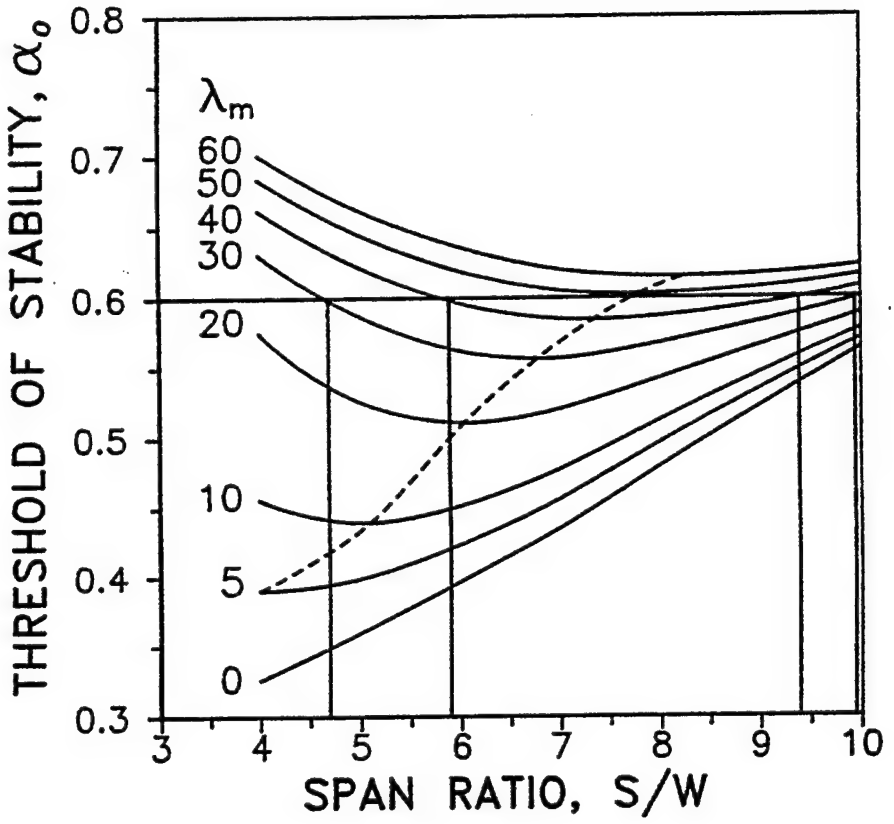

Figure 4. Stability Threshold Crack Length, α_o, for Three-Point Bend Specimens With Span-to-Width Ratios Ranging From 4 to 10. The Dimensionless Machine Compliance Varies From 0 to 60. The Dashed Line Indicates the Conditions of Our Test Setup.

3. Experimental Procedure

3.1 Material. A hot-pressed silicon nitride (NC132, Norton Co., Worcester, MA) was used for the fracture toughness tests. The material has a maximum grain size of 3 μm. The room-

temperature properties as reported by the manufacturer are density 3.25 g/cm^3, modulus of rupture 825±137 MPa, Vicker's hardness 16 GPa, Young's modulus 3.2×10^5 MPa, and Poisson's ratio 0.27. The fracture toughness of NC 132 has been determined by several techniques [25–29], and the results are summarized in Table 1.

Table 1. Fracture Toughness of NC132 Measured by Several Methods

Test Method	K_{IC}, Mpa $\sqrt{m}$	Reference
Indentation	4.0	Anstis et al. [25]
Controlled Flaw (Surface Crack in Flexure)	4.6	Chantikal et al. [26]
Chevron Notch	4.7	Salem and Shannon [27]
Double Cantilever Beam	4.9	Evans and Charles [28]
Constant Moment Double Cantilever Beam	4.0	Freiman et al. [29]

Some of these methods most likely included some stable crack extension, such as the constant-moment-double-cantilever-beam test and chevron notch. The controlled flaw test, on the other hand, most likely did not exhibit stable crack extension.

The material was cut into 6-mm × 8-mm × 45-mm bend bar specimens with the hot-pressing direction perpendicular to the long direction of the specimen and parallel to the crack plane. All specimens were carefully polished on the side and top surfaces, first on 9-μm and 6-μm diamond bonded wheels and then with 3-μm and 1-μm diamond paste.

3.2 Machine Compliance. The stability calculations were used as a guideline in designing a test system that would be stiff enough so that stable and unstable crack growth could be realized. The testing arrangement consisted of an Instron 250-kN servo-hydraulic load frame with a 25-kN load cell connected to a 250-kN load cell. The manufacturer's specifications for this arrangement are as follows:

Frame stiffness:	585 kN/mm	(3.27×10^6 lb/in)
Load cell stiffness, 250 kN:	2,560 kN/mm	(14.3×10^6 lb/in)
Load cell stiffness, 25 kN:	1,020 kN/mm	(5.7×10^6 lb/in).

The resulting stiffness of the frame with the two load cells was calculated as 322 kN/mm (1.8×10^6 lb/in).

Initially, a commercially available bend fixture was used. However, with this setup, stable crack growth was unattainable even for very long cracks. The stability analysis, which provided guidance to the experiments, indicated that the fixture had to be further stiffened for stability to be obtained in this system. Thus this fixture was replaced by a stiffer one. The compliance of the machine, load cells, and fixturing arrangement was determined experimentally using an uncracked silicon nitride bend bar. The measured compliance of this test setup was 3.07×10^{-8} m/N, which gave a stiffness of 32.57 kN/mm (1.86×10^5 lb/in). This measured compliance corresponded to a dimensionless compliance $\lambda_m = 58.9$.

One specimen with a crack length of a/W = 0.75 was tested an a more compliant articulating fixture, in order to document the effect of the greater machine compliance.

3.3 Test Procedure. The specimens were indented with a Vicker's indenter using loads ranging from 69 to 490 N. These specimens were then loaded in the bridge indentation compression fixture [19] creating straight precracks. Crack length was measured on both side surfaces. The higher indent loads were employed to create the shorter cracks (< 0.6 a/W), while the lower loads were used to create the longer cracks.

The fracture toughness tests were performed in three-point bending with a span of 40-mm and an S/W ratio of 5. The tests were displacement controlled at a displacement rate of 1.7 μm/s. The load resolution was approximately 2 N.

4. Results and Discussion

4.1 Stability. The stability analysis predicted a critical crack length of a/W = 0.66 for the compliance measured for our test setup (see Figure 3). Correspondingly, the load displacement

records clearly differed for different crack length regimes, even though the crack length regimes overlap somewhat.

The load-vs.-displacement record was linear to the point of fracture as shown in Figure 5a (unstable) for crack lengths far below the threshold value ($0.26 < a/W < 0.56$). Fracture occurred instantaneously across the whole cross section, as shown in the fractographic example in Figure 7a.

Some stable crack extension occurred prior to either fracture or a large crack jump for crack lengths close to the critical crack length ($0.53 < a/W < 0.67$). This is documented on the load displacement record as nonlinearity near the maximum load followed by a steep load drop to a low load value (see Figure 5b, semistable).

A completely stable load displacement curve (Figure 6a, stable) or, more typically, a curve with pop-ins, as shown in Figure 6b, was observed for specimens with very long cracks ($0.62 < a/W < 0.78$). This curve shows significant nonlinearity or several short crack pop-in jumps followed by one or several larger pop-in jumps. The larger crack jumps differ from those observed in the previous group, however, in that they exhibit clear crack arrest at some *intermediate* load value.

Evidence of partially stable crack propagation or crack jumps can be observed on the fracture surface as shown in Figure 7b, which is the specimen corresponding to the load displacement record shown in Figure 6b (pop-in).

4.2 Fracture Toughness. Fracture toughness as a function of precrack length is shown in Figure 8. The fracture toughness values vary from a high of 4.65 MPa$\sqrt{m}$ to a low of 4.00 MPa$\sqrt{m}$. It can be seen that for short precrack lengths and correspondingly low specimen compliances the measured fracture toughness values are higher than for longer precracks. A similar trend had been observed before for tungsten [17] and PMMA [16].

The fracture toughness values are summarized in Table 2 grouped by stability. Figure 8 displays these results graphically including also the predicted critical crack length for which the transition

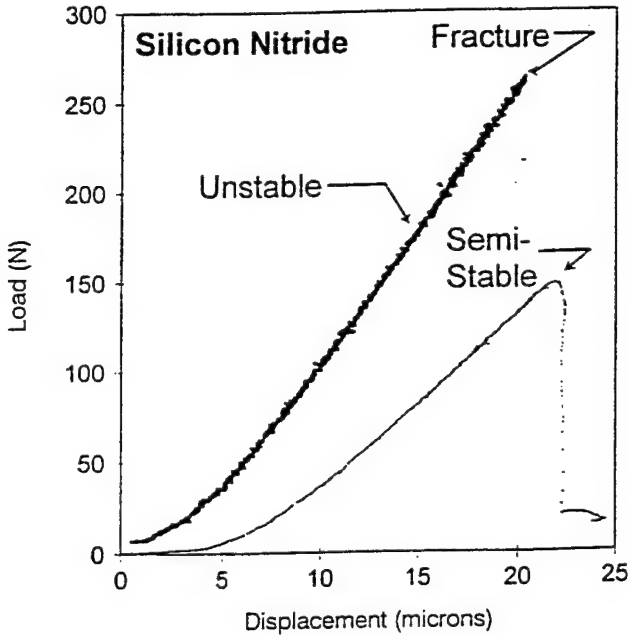

Figure 5. Load-Displacement Records for Silicon Nitride Specimens Showing (a) Unstable Fracture - Typical for $0.26 < \alpha < 0.56$, or (b) Semistable Fracture - Typical for $0.53 < \alpha < 0.67$.

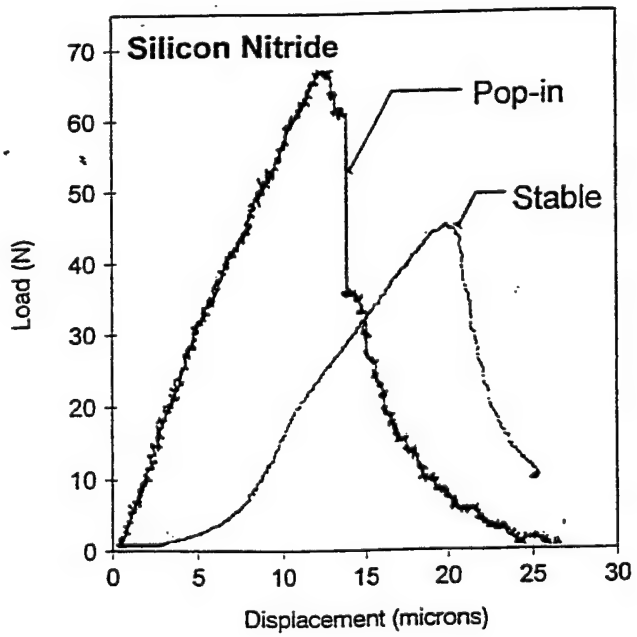

Figure 6. Load-Displacement Records for Silicon Nitride Specimens Showing (a) Stable Fracture or (b) Stable Fracture With Pop-In. These Specimens Were Precracked to $0.62 < \alpha < 0.78$. Note That the Crack Arrests After a Short Crack Extension.

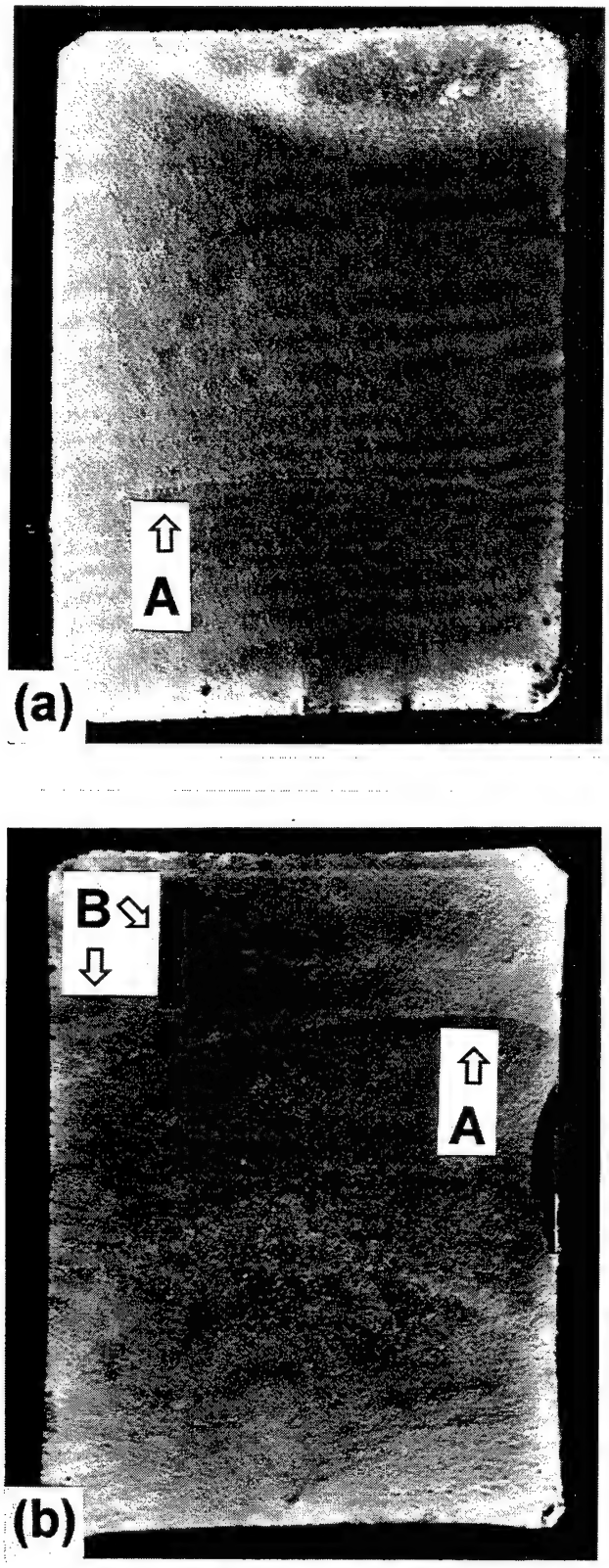

Figure 7. Typical Fractographs Showing Crackfront of Precrack at A and Pop-In Crack(s) at B for (a) Unstable and (b) Stable Fracture.

Table 2. Fracture Toughness by the SEPB Method for Varying Degrees of Stability

NC132	Unstable	Semistable	Stable Including Pop-Ins
K_{IC} (Mpa$\sqrt{m}$)	4.54±0.12	4.23±0.13	4.19±0.08
No. of Tests	7	5	5
a/W	0.26–0.56	0.53–0.65	0.64–0.78

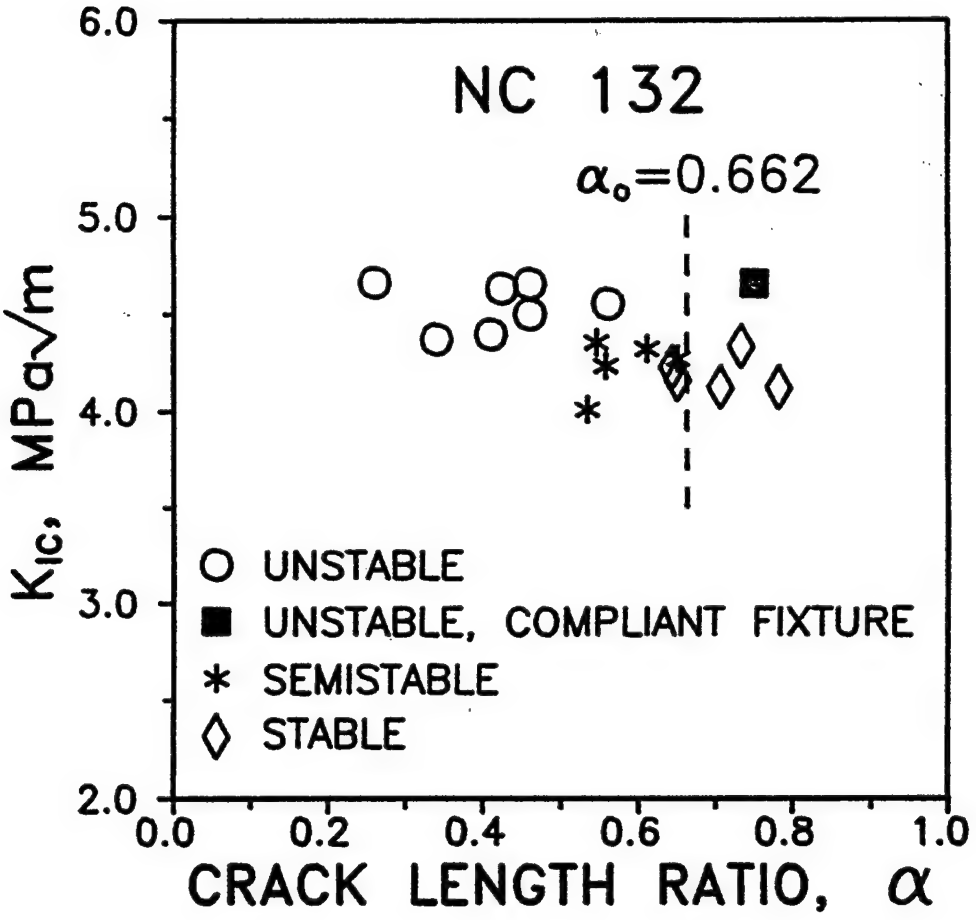

Figure 8. Fracture Toughness Measured for Specimens of Varying Precrack Length. The Type of Load Displacement Is Indicated. The Dashed Line Indicates the Analytically Determined Crack Length Which Separates the Unstable Regime (Shorter Precracks) From the Stable Regime.

from unstable to stable behavior should occur. It can be seen that the predicted crack length, α_0 = 0.66 at stability, shown by the vertical line in Figure 8, agrees well with the transition observed in the experiments.

Four specimens with a/W > 0.7 were tested. Three were tested on the stiff fixture, and one was tested on a more compliant fixture. The specimens tested on the stiff fixture all showed stable load displacement curves, and the resulting mean fracture toughness value was 4.10 Mpa$\sqrt{m}$. The specimen tested on the more compliant fixture resulted in an unstable load-displacement curve, and the fracture toughness value was 4.65 Mpa$\sqrt{m}$. This value agrees with the fracture toughness values obtained for the other unstable tests. Using the more compliant fixture increases the overall machine compliance to a value much above 59. For higher machine compliace values, the analysis predicts a larger threshold crack length (Figure 2) or complete instability. Thus this setup was expected to result in unstable fracture. This was borne out by the observed load-displacement trace and the higher fracture toughness value.

Table 2 and Figure 8 also indicate that the fracture toughness measured for the onset of unstable fracture is about 10% higher than that measured from a stably propagating crack. This trend agrees with previous observations by Baratta and Dunlay [16] and Underwood et al. [17].

A test of means was performed, in order to decide if the difference between the stable and unstable fracture toughness values was significant. For this test, the fracture toughness values of the five semistable specimens and the five stable specimens were combined for the calculation of their mean. This combined mean was compared to the mean of seven unstable specimens. The rational for this is that the mean of the fracture of the semistable is slightly higher than that of the stable specimen, and this combined mean, when compared to that of the unstable specimens, would provide a more conservative result. The mean of the fracture toughness of the unstably fractured specimens differed from that of the combined mean of the semistably and stably fractured specimens at the 99.5% confidence level.

It could be argued that the difference in measured fracture toughness between the shorter and longer cracks is due to the residual tensile stress field caused by the indent. Several researchers have pointed out that such an effect might exist [30, 31]. However, the indents for the shorter precracks were created using higher indent loads (250–500 N) while the longer precracks were created using lower loads (70–200 N). The contribution to the stress intensity from the residual stress due to indentation, K_{res}, should be calculated by considering a wedge load at the indent point. Since the details of the applied load are unknown, K_{res} can be calculated from an empirical formulation for a semicircular crack [32] as:

$$K_{res} = \chi\,(E/H)^{1/2}\,P/(c_0)^{3/2}, \tag{7}$$

where E is the elastic modulus, H is the hardness, c_0 is the crack length, P is the indentation load, and χ is a constant. This K_{res} can be taken as an upper bound for the precracked beam, since the introduction of the straight pop-in crack will reduce the extent of K_{res}.

K_{res} acts to reduce the measured fracture toughness values and decreases with crack length for constant indent load. Thus, if a correction for residual stress were included, the difference between the fracture toughness measured from cracks propagating under stable and unstable conditions would be even more pronounced.

The results of the stability analysis can be generalized to provide guidance for fracture toughness tests of brittle materials. The family of curves shown in Figure 4, which can be considered generally applicable to brittle materials, shows the threshold stability parameter, α_0, as a function of span ratio, S/W, and normalized machine compliance, λ_m. The dashed line in the figure connects the minimum points of this family of stability curves. If α_0 is chosen to be greater than the minimum value, then stability is predicted for each given λ_m and S/W. However, a practical consideration for α_0 should be that it is no greater than 0.60. The reasoning here is that the stress intensity curve rises markedly when a/W is greater than 0.60 (see equation 5), and even small measurement errors of the crack length will result in a large error in the subsequent fracture toughness calculation. Thus, a horizontal line is drawn in Figure 4 at $\alpha_0 = 0.60$ to provide guidance in choosing α_0 and S/W as a function of λ_m.

Notice that in Figure 4 the stability curve of $\lambda_m = 50$ becomes tangent to the horizontal line for $\alpha_0 = 0.60$. Therefore, to retain stability, λ_m must be chosen to be less than 50. The horizontal line for $\alpha_0 = 0.60$ intercepts the λ_m curve of 40 at S/W = 5.9 and 9.4; and the curve of $\lambda_m = 30$ at S/W = 4.7 and 9.9. The normalized machine compliance of 40 and 30 can be realized for the HPSN material tested in this study by reducing the B dimension from 6 mm used in this work to 4 mm and 3 mm, respectively, resulting in a beam cross section of 8 mm × 4 mm or 8 mm × 3 mm.* Alternatively, a width-to-thickness ratio, W/B, of 2 or 2.27 could be selected with appropriate adjustments in K expressions. It is expected that a normalized machine compliance of less than 30 will be difficult to attain in a practical manner for most structural ceramic materials which have a large Young's modulus. Therefore, only data taken from Figure 4 for $\lambda_m = 40$ and 30 are included in the guideline for stable fracture toughness testing. Table 3 summarizes the recommended beam geometries to ensure stable fracture. Note that for practical consideration, such as minimizing specimen deflection and optimizing specimen volume, beam span ratios should be no greater than 7.5 or 8.

Table 3. Recommended Beam Geometries to Ensure Stable Fracture[a]

λ_m	S/W Range for $\alpha_0 \leq 0.60$	Optimum S/W	Minimum α_0	W (mm)	B (mm)
40	5.9–9.4	7.4	0.58	6.0	4.0
30	4.7–9.9	6.8	0.56	6.0	3.0

[a] For a test system with a machine compliance (including fixture) of 3.0×10^{-8} m/N.

Nakayama [8] has suggested an explanation of what appears to be an artificial increase in fracture energy associated with unstable fracture as compared to stable fracture. The mechanism presented was based on energy considerations, where the total elastic energy stored in the system at the time of fracture is composed of both the energy in the specimen and the energy in the testing apparatus. He further considers the effective fracture energy required to separate beam specimen. Since the

* These latter beam dimensions will require improved load resolution, since fracture load will be relatively low.

elastic energy stored at the time of the fracture is dissipated by the fracture process, the difference in energy obtained by subtracting the effective fracture energy from the total energy in the system at the time of fracture provides a criterion of the mode of fracture. When this difference is greater than zero, the mode of fracture is catastrophic, because excess energy must be consumed by other forms of energy, e.g., the kinetic energies of fragments. Alternatively, if the energy stored is not enough to complete the fracture process and additional external work is required, the mode of fracture may then be stable. Nakayama [8] further stated: "The exact measurement of the effective fracture energy is valid only for perfectly stable fractures." At the time Nakayama published his report, an analysis which could predict stable fracture for brittle materials was not available. Subsequently, other researchers, as indicated in the Introduction, have provided such analyses, which have defined stable and unstable fracture in terms of the appropriate beam geometry, materials, and testing machine parameter. All of these reports use energy considerations, i.e., energy release rate, including that given by Bluhm [10], which was the basis for prediction of stability given by equation 6 presented in this study, resulting in Figures 2, 3, and 4. Nakayama [8] further draws on an analogy to aid the reader in understanding this phenomenon by stating: "The present method resembles the Charpy impact test in which the entire energy consumed in bending fracture is measured by a decrease on the maximum height of swing of the pendulum after it has broken the specimen. The mechanism in this test, however, is dynamic, and the fragments of the specimen, after fracture, carry considerable excess kinetic energy. Separation of the effective energy from the kinetic energy is impossible in the Charpy test . . . ." The present method corresponds in principle to the Charpy test in that the impacting speed of the pendulum is extremely small and the mass is quite large. The accuracy of measurement in such an extreme situation is very low in the Charpy test.

5. Conclusions

(1) Stability parameters were calculated for the rectangular beam loaded in three-point bending under plane strain conditions. Beam span ratios ranging from 4 to 10 were considered.

(2) A stability threshold crack length, α_0, was calculated for a span ratio of S/W = 5 predicting the transition from unstable to stable crack extension as the precrack length is increased.

(3) Fracture toughness values were measured for hot-pressed silicon nitride bend bars with varying precrack lengths using a stiff test system.

(4) A transition from unstable to stable crack extension was observed in agreement with the theoretical predictions.

(5) The fracture toughness values measured for stable crack extension were about 10% lower than those measured for unstable crack extension.

(6) The mean of the fracture toughness of unstably fractured specimens differed significantly from that of the combined semistably and stably fractured specimens. Thus, it can be concluded that unstable fracture of hot-pressed silicon nitride (NC 132) will give rise to an artificial increase in fracture toughness of about 10%.

6. Recommendation

Beam geometry, beam span ratios, initial threshold crack length ratios, and machine compliance values are recommended to aid in realizing stable crack growth during fracture toughness testing of three-point loaded beams.

It is recommended that:

(1) Beam geometry, beam span ratios, initial threshold crack length ratios, machine Compliances values, and beam materials, i.e., Young's modulus of elasticity, be considered in realizing stable crack growth during fracture testing of beam specimens.

(2) Examination of other structural ceramic materials be concluded to determine the extent of the increase in fracture toughness occurring during unstable extension. If such increases are considerable, then stable crack extension should be seriously considered when attempting to determine fracture toughness of these brittle materials.

INTENTIONALLY LEFT BLANK.

7. References

1. Freiman, S. W. "A Critical Evaluation of Fracture Mechanics Techniques for Brittle Materials." *Fracture Mechanics of Ceramics*, vol. 6, pp. 27–45, edited by R. C. Bradt, A. G. Evans, D. P. H. Hasselman, and F. F. Lange, New York: Plenum Press, 1983.

2. American Society for Testing and Materials. "Terminology Relating to Fracture Testing." ASTM Standard E 616-89, *ASTM Annual Book of Standards*, vol. 03.01, pp. 647–58, Philadelphia, PA, 1993.

3. American Society for Testing and Materials. "Standard Test Methods for Plane-Strain Fracture Toughness of Metallic Materials," ASTM STD E399, *Annual Book of ASTM Standards*, Philadelphia, PA, 1990.

4. Srawley, J. E., and W. F. Brown Jr. "Fracture Toughness Testing Methods." *Fracture Toughness Testing and Its Applications*, ASTM STP 381, pp. 133–198, American Society for Testing and Materials, Philadelphia, PA, 1965.

5. Brown, W. F., Jr., and J. E. Srawley. *Plane Strain Crack Toughness Testing of High Strength Metallic Materials*. ASTM STP 410, American Society for Testing and Materials, Philadelphia, PA, 1969.

6. Wiederhorn, S. M. "Reliability, Life Prediction, and Proof Testing of Ceramics." *Ceramics for High Performance Applications*, pp. 633–63, edited by J. J. Burke, A. E. Gorum, and R. N. Katz, Chestnuthill, MA: Brook Hill Publishing Co., 1974.

7. Suresh, S., T. Nakamura, Y. Yeshurun, K. -H. Yang, and J. Duffy. "Tensile Fracture Toughness of Ceramic Materials: Effects of Dynamic loading and Elevated Temperatures." *J. Am. Ceram. Soc.*, vol. 73, no. 8, pp. 2457–66, 1990.

8. Nakayama, J. "Direct Measurement of Fracture Energies of Brittle Heterogeneous Materials." *J. Am. Ceram. Soc.*, vol. 48, no. 11, pp. 538–87, 1965.

9. Clausing, D. P. "Crack Stability in Linear Elastic Fracture Mechanics." *Int. J. Fract. Mech.*, vol. 5, no. 3, pp. 211–26, 1969.

10. Bluhm, J. I. "Stability Considerations in the Three Dimensional Work of Fracture Specimens." *Proceedings of the Fourth International Conference on Fracture*, pp. 409–17, edited by D. M. R. Taplin, Waterloo, Ontario, Canada: University of Waterloo Press, 1977.

11. Schimoeller, H. A. "An Elastic-Quasistatic Crack Stability Criterion of Fracture Mechanic Specimens Investigated by Displacement-Controlled Closed Loop Testing Systems." *Int. J. Fract.*, vol. 12, no. 3, pp. 481–84, 1976.

12. Tatersall, H. G., and G. J. Tappin. "The Work of Fracture and its Measurement in Metals, Ceramics and Other Materials." *J. Mater. Sci.*, vol. 1, pp. 296–301, 1960.

13. Bluhm, J. I. "Slice Synthesis of a Three Dimensional 'Work of Fracture' Specimen." *Eng. Fract. Mech.*, vol. 7, pp. 593–604, 1975.

14. Cooper, G. A. "Optimization of the Three-Point Bend Test for Fracture Energy Measurement." *J. Mater. Sci.*, vol. 12, pp. 277–89, 1977.

15. Mai, Y. W., and A. G. Atkins. "Crack Stability in Fracture Toughness Testing." *J. Strain. Anal.*, vol. 15, no. 2, pp. 63–74, 1980.

16. Baratta, F. I., and W. A. Dunlay. "Crack Stability in Simply Supported Four-Point and Three-Point Loaded Beams of Brittle Materials." *Mech. Mater.*, vol. 10, pp. 149–59, 1990.

17. Underwood, J. H., F. I. Baratta, and J. J. Zalinka. "Fracture-Toughness Tests and Displacement and Crack-Stability Analysis of Tungsten Round Bend Specimens." *Exp. Mech.*, vol. 31, no. 4, pp. 353–59, 1991.

18. Sigl, L. S. "On the Stability of Cracks in Flexure Specimens." *Int. J. Fract.*, vol. 51, pp. 241–54, 1991.

19. Nose, T., and T. Fujii. "Evaluation of Fracture Toughness for Ceramic Materials by a Single-Precracked Beam Method." *J. Am. Ceram. Soc.*, vol. 71, no. 5, pp. 328–33, 1988.

20. Bar-On, I., J. T. Beals, G. L. Leatherman, and C. M. Murray. "Fracture Toughness of Precracked Bend Bars." *J. Am. Ceram. Soc.*, vol. 73, no. 8, pp. 2519–22, 1990.

21. Choi, S. R., A. Chulya, and J. A. Salem. "Analysis of Precracking Parameters for Ceramic Single-Edge-Precracked-Beam Specimens." *Fracture Mechanics of Ceramics*, vol. 10, pp. 73–78, edited by Sakai, New York: Plenum Press, 1992.

22. Baratta, F. I. "Load-Point Compliance of a Three-Point Loaded Cracked-Notched Beam." JTEV, vol. 16, no. 7, pp. 59–71, 1988.

23. Baratta, F. I., and J. H. Underwood. "Notch Dimensions for Three-Point Bend Fracture Specimens Based on Compliance Analyses." *JTEV*, vol. 20, no. 5, pp. 343–48, 1992.

24. Private discussion with C. P. Freese of the U.S. Army Research Laboratory, Aberdeen Proving Ground, MD, 1995.

25. Anstis, G. R., P. Chantikul, B. R. Lawn, and D. B. Marshall. "Critical Evaluation of Indentation Techniques for Measuring Fracture Toughness: I, Direct Crack Measurements." *J. Am. Ceram. Soc.*, vol. 64, no. 9, pp. 533–38, 1981.

26. Chantikul, P., G. R. Anstis, B. R. Lawn, and D. B. Marshall. "A Critical Evaluation of Indentation Techniques for Measuring Fracture Toughness: II, Strength Method." *J. Am. Ceram. Soc.*, vol. 64, no. 9, pp. 539–43, 1981.

27. Salem, J. A., and J. L. Shannon Jr. "Fracture Toughness of Si_3N_4 Measured With Short Bar Chevron Notched Specimens." *J. Mater. Sci.*, vol. 22, pp. 321–24, 1987.

28. Evans, A. G., and E. A. Charles. "Fracture Toughness Determination by Indentation." *J. Am. Ceram. Soc.-Discussions and Notes*, vol. 59, nos. 7–8, pp. 371–72, 1976.

29. Freiman, S. W., A. Williams, J. J. Mecholsky, and R. W. Rice. "Fracture of Si_3N_4 and SiC." *Ceramic Microstructures 76*, pp. 824–34, edited by R. M. Fulrath and J. A. Pask, Boulder, CO: Westview Press, Inc., 1977.

30. Warren, R., and B. Johannesson. "Creation of Stable Cracks in Hardmetals Using 'Bridge' Indentation." *Powder Metall.*, vol. 27, no. 1, pp. 25–29, 1984.

31. Nishida, T., T. Shiono, and T. Nishikawa. "On the Fracture Toughness of Polycrystalline Alumina Measured by SEPB Method." *J. Eur. Ceram. Soc.*, vol. 5, pp. 379–83, 1989.

32. Lawn, B. R., A. G. Evans, and D. B. Marshall. "Elastic/Plastic Indentation in Ceramics: The Median/Radial Crack System." *J. Am. Ceram. Soc.*, vol. 63, nos. 9–10, pp. 574–81, 1980.

INTENTIONALLY LEFT BLANK.

Appendix A:

Load-Point Compliance and Stress Intensity Relationships

INTENTIONALLY LEFT BLANK.

Consider Figure 1 (in the text of the report) showing the geometry of the center loaded beam. The deflection at the point of load application is defined as

$$\delta_s = \delta + \Delta\delta, \tag{A-1}$$

where δ_s is the deflection at the point of load application due to both the deflection of the uncracked beam and that contributed by the presence of the crack $\Delta\delta$. Timoshenko,[1] from strength of materials considerations, gives the deflection of such a solid beam as

$$\delta = 2\frac{P}{EB}(S/2W)^2 (S/2W) + [2.85(S/2W) - 0.42/(S/2W)^2]/4. \tag{A-2}$$

The deflection of the beam caused by the presence of the crack is defined as

$$\Delta\delta = \frac{W\partial}{\partial P}\left(B\int_0^{\alpha} G_I \, d\alpha\right), \tag{A-3}$$

where P is the applied load, $\alpha = a/W$, G_I is the Mode I, plane-strain energy release rate, which, given in terms of Mode I, stress intensity factor, K_I, and modulus of elasticity, E, is

$$G_I = (1 - \nu^2) K_I^2/E. \tag{A-4}$$

K_I for the beam shown in Figure 1 is defined as

$$K_I = \frac{6Ma^{1/2}}{BW^2}[f(\alpha)], \tag{A-5}$$

---

[1]Timoshenko, S. Strength of Materials, Part I. New York: D. Van Nostrand Co., 1958.

where M is the appropriate bending moment, a is the crack length, B is the beam width, W is the beam height, and [f (α)] is the polynomial:

$$[f(\alpha)] = A_o + A_1\alpha + A_2\alpha^2 + A_3\alpha^3 + A_4\alpha^4 + A_5\alpha^5 + A_6\alpha^6. \qquad \text{(A-6)}$$

The previous coefficients are given in the text for S/W = 5.

Substitution of equation A-5 into A-4, this, in turn, into equation A-3, and differentiating with respect to the applied load, gives the additional displacement due to the presence of the crack as

$$\Delta\delta = \frac{18\ (S/2\,W)^2}{EB}\ (1 - \nu^2)\ \int_0^{\alpha} \alpha\ [f(\alpha)]^2\ d\alpha, \qquad 0 \leq \alpha\ 0.070. \qquad \text{(A-7)}$$

Adding the displacement caused by the uncracked beam, equation A-2, to that of the cracked beam, equation A-7, gives the total deflection of the specimen in terms of compliance; which is summarized in equation 3 in the body of the report.

Appendix B:

Wide-Range Stress Intensity Factor

INTENTIONALLY LEFT BLANK.

As mentioned in the text, the wide-range stress intensity formulations also obtained from the numerical data of Baratta and Underwood[1] are given in the following for three-point loaded beams having span ratios of 4, 5, 6, 7, 8, and 10, as well as for the constant moment beam.

$$K_I = \frac{(3/2)PS}{BW^{3/2}} \frac{\alpha^{1/2}}{(1-\alpha)^{3/2}} [f(\alpha)] \tag{B-1}$$

and

$$K_I = \frac{6M}{BW^{3/2}} \frac{\alpha^{1/2}}{(1-\alpha)^{3/2}} [f(\alpha)], \tag{B-2}$$

where equations B-1 and B-2 are for the three-point and constant moment loaded beam, respectively. Also [f (α)] is given by the following polynomial expression:

$$[f(\alpha)] = A_o + A_1\alpha + A_2\alpha^2 + A_3\alpha^3 + A_4\alpha^4 + A_5\alpha^5. \tag{B-3}$$

The coefficients A_0, A_1, A_2, . . . A_5 are presented in Table B-1. The previous equations are accurate to + 1.5% and have a wide range of $0 \le \alpha \le 1.0$.

Table B-1. Coefficients for the Polynomial f (α) Three-Point Loaded and Constant Moment Beam

	S/W						Constant Moment
	4	5	6	7	8	10	M = C
A_0	1.8931	1.9109	1.9230	1.9322	1.9381	1.9472	1.9820
A_1	-5.2029	-5.1552	-5.1389	-5.1007	-5.0947	-5.0247	-4.9828
A_2	12.9411	12.6880	12.6194	12.3861	12.3861	11.8954	11.8279
A_3	-19.9433	-19.5736	-19.5510	-19.0071	-19.2142	-18.0635	-18.4764
A_4	16.1869	15.9377	15.9841	15.4677	15.7747	14.5986	15.3440
A_5	-5.2122	-5.1454	-5.1736	-4.9913	-5.1270	-4.8696	-5.0316

[1]Baratta, F. I., and J. H. Underwood. "Notch Dimensions for Three-Point Bend Fracture Specimens Based on Compliance Analyses." *JTEV*, vol. 20, no. 5, pp. 343–48, 1992.

INTENTIONALLY LEFT BLANK.

NO. OF COPIES	ORGANIZATION
2	DEFENSE TECHNICAL INFORMATION CENTER DTIC DDA 8725 JOHN J KINGMAN RD STE 0944 FT BELVOIR VA 22060-6218
1	HQDA DAMO FDQ DENNIS SCHMIDT 400 ARMY PENTAGON WASHINGTON DC 20310-0460
1	CECOM SP & TRRSTRL COMMCTN DIV AMSEL RD ST MC M H SOICHER FT MONMOUTH NJ 07703-5203
1	PRIN DPTY FOR TCHNLGY HQ US ARMY MATCOM AMCDCG T M FISETTE 5001 EISENHOWER AVE ALEXANDRIA VA 22333-0001
1	PRIN DPTY FOR ACQUSTN HQS US ARMY MATCOM AMCDCG A D ADAMS 5001 EISENHOWER AVE ALEXANDRIA VA 22333-0001
1	DPTY CG FOR RDE HQS US ARMY MATCOM AMCRD BG BEAUCHAMP 5001 EISENHOWER AVE ALEXANDRIA VA 22333-0001
1	ASST DPTY CG FOR RDE HQS US ARMY MATCOM AMCRD COL S MANESS 5001 EISENHOWER AVE ALEXANDRIA VA 22333-0001

NO. OF COPIES	ORGANIZATION
1	DPTY ASSIST SCY FOR R&T SARD TT F MILTON THE PENTAGON RM 3E479 WASHINGTON DC 20310-0103
1	DPTY ASSIST SCY FOR R&T SARD TT D CHAIT THE PENTAGON WASHINGTON DC 20310-0103
1	DPTY ASSIST SCY FOR R&T SARD TT K KOMINOS THE PENTAGON WASHINGTON DC 20310-0103
1	DPTY ASSIST SCY FOR R&T SARD TT B REISMAN THE PENTAGON WASHINGTON DC 20310-0103
1	DPTY ASSIST SCY FOR R&T SARD TT T KILLION THE PENTAGON WASHINGTON DC 20310-0103
1	OSD OUSD(A&T)/ODDDR&E(R) J LUPO THE PENTAGON WASHINGTON DC 20301-7100
1	ARL ELECTROMAG GROUP CAMPUS MAIL CODE F0250 A TUCKER UNIVERSITY OF TX AUSTIN TX 78712
1	DUSD SPACE 1E765 J G MCNEFF 3900 DEFENSE PENTAGON WASHINGTON DC 20301-3900
1	USAASA MOAS AI W PARRON 9325 GUNSTON RD STE N319 FT BELVOIR VA 22060-5582

NO. OF COPIES ORGANIZATION

1 CECOM
PM GPS COL S YOUNG
FT MONMOUTH NJ 07703

1 GPS JOINT PROG OFC DIR
COL J CLAY
2435 VELA WAY STE 1613
LOS ANGELES AFB CA 90245-5500

1 ELECTRONIC SYS DIV DIR
CECOM RDEC
J NIEMELA
FT MONMOUTH NJ 07703

3 DARPA
L STOTTS
J PENNELLA
B KASPAR
3701 N FAIRFAX DR
ARLINGTON VA 22203-1714

1 SPCL ASST TO WING CMNDR
50SW/CCX
CAPT P H BERNSTEIN
300 O'MALLEY AVE STE 20
FALCON AFB CO 80912-3020

1 USAF SMC/CED
DMA/JPO
M ISON
2435 VELA WAY STE 1613
LOS ANGELES AFB CA 90245-5500

1 US MILITARY ACADEMY
MATH SCI CTR OF EXCELLENCE
DEPT OF MATHEMATICAL SCI
MDN A MAJ DON ENGEN
THAYER HALL
WEST POINT NY 10996-1786

1 DIRECTOR
US ARMY RESEARCH LAB
AMSRL CS AL TP
2800 POWDER MILL RD
ADELPHI MD 20783-1145

NO. OF COPIES ORGANIZATION

1 DIRECTOR
US ARMY RESEARCH LAB
AMSRL CS AL TA
2800 POWDER MILL RD
ADELPHI MD 20783-1145

3 DIRECTOR
US ARMY RESEARCH LAB
AMSRL CI LL
2800 POWDER MILL RD
ADELPHI MD 20783-1145

ABERDEEN PROVING GROUND

2 DIR USARL
AMSRL CI LP (305)

NO. OF COPIES	ORGANIZATION
1	COMMANDER US ARMY RESEARCH OFC INFO PROCESSING OFC PO BOX 12211 RESEARCH TRIANGLE PARK NC 27709-2211
1	COMMANDER USAMC AMCSCI 5001 EISENHOWER AVE ALEXANDRIA VA 22333
2	COMMANDER US ARMY ARDEC TECH LIB DR K WILLISON PICATINNY ARSENAL NJ 07806-5000
1	COMMANDER US ARMY TACOM AMSTA TSL TECH LIB WARREN MI 48297-5000
1	NATL INST OF STANDARDS & TECH GEORGE QUINN CERAMICS DIV BLDG 223 A326 GAITHERSBURG MD 02899
14	WORCESTER POLYTECH INST DR R BIEDERMAN DR R SISSON DR ISA BAR-ON (10 CPS) DR MARINA PASCUCCI DR R NATHAN KATZ 100 INSTITUTE RD WORCESTER MA 01609
1	MIAC/CINDAS PURDUE UNIVERSITY 2595 YEAGER RD WEST LAFAYETTE IN 47905

NO. OF COPIES	ORGANIZATION
3	MATERIALS MODIFICATION INC DR T S SUDARSHAN DR SANG YOO RESHINA KUMAR 2929-P1 ESKRIDGE RD FAIRFAX VA 22031
1	CERCOM INC DR JAMES SHIH 1960 WATSON WAY VISTA CA 92083
10	MR FRANCIS BARATTA 138 RIDGE ST ARLINGTON MA 02174-1737
	ABERDEEN PROVING GROUND
27	DIR USARL AMSRL WM M DR DENNIS VIECHNCKI AMSRL WM MC DR THOMAS V HYNES DR JOSEPH WELLS JEFFREY J SWAB GARY A GILDE DR JERRY LASALVIA AMSRL WM MD ROBERT DOWDING KYU CHO (20 CPS)
1	DIR USAMSAA AMXSY MP

INTENTIONALLY LEFT BLANK.

REPORT DOCUMENTATION PAGE

Form Approved
OMB No. 0704-0188

1. AGENCY USE ONLY *(Leave blank)*	2. REPORT DATE	3. REPORT TYPE AND DATES COVERED
	June 1997	Final, Oct 94 - Sep 96

4. TITLE AND SUBTITLE

Crack Stability and Its Effect on Single-Edge-Precracked-Beam (SEPB) Fracture Toughness of Hot-Pressed Silicon Nitride Beam Specimens

5. FUNDING NUMBERS

44LAL
552LBA

6. AUTHOR(S)

Isa Bar-On,* Francis I. Baratta, and Kyu Cho

7. PERFORMING ORGANIZATION NAME(S) AND ADDRESS(ES)

U.S. Army Research Laboratory
ATTN: AMSRL-WM-MD
Aberdeen Proving Ground, MD 21005-5066

8. PERFORMING ORGANIZATION REPORT NUMBER

ARL-TR-1407

9. SPONSORING/MONITORING AGENCY NAMES(S) AND ADDRESS(ES)

10.SPONSORING/MONITORING AGENCY REPORT NUMBER

11. SUPPLEMENTARY NOTES

* Worcester Polytechnic Institute, Mechanical Engineering Department, Worcester, MA 01609.
Also published in *Journal of the American Ceramic Society*, 79 [9], 2300-308 (1996).

12a. DISTRIBUTION/AVAILABILITY STATEMENT

Approved for public release; distribution is unlimited

12b. DISTRIBUTION CODE

13. ABSTRACT *(Maximum 200 words)*

The effect of stable crack extension on fracture toughness test results was determined using single-edge-precracked-beam specimens. Crack growth stability was examined theoretically for bars loaded in three-point bending under displacement control. The calculations took into account the stiffness of both the specimen and the loading system. The results indicated that the stiffness of the testing system played a major role in crack growth stability. Accordingly, a test system and specimen dimensions were selected which would result in unstable or stable crack extension during the fracture toughness test depending on the exact test conditions. Hot-pressed silicon nitride bend bars (NC132) were prepared with precracks of different lengths resulting in specimens with different stiffnesses. The specimens with the shorter precracks and thus higher stiffness broke without stable crack extension, while those with long cracks, and lower stiffness broke after some stable crack extension. The fracture toughness values from the unstable tests were 10% higher than those from the stable tests. This difference, albeit small, is systematic and is not considered to be due to material or specimen-to-specimen variation. It is concluded that instability due to the stiffness of the test system and specimen must be minimized to ensure some stable crack extension in a fracture toughness test of brittle materials in order to avoid inflated fracture toughness values.

14. SUBJECT TERMS

crack stability, SEPB fracture toughness, Si3N4 (silicon nitride)

15. NUMBER OF PAGES

42

16. PRICE CODE

17. SECURITY CLASSIFICATION OF REPORT	18. SECURITY CLASSIFICATION OF THIS PAGE	19. SECURITY CLASSIFICATION OF ABSTRACT	20. LIMITATION OF ABSTRACT
UNCLASSIFIED	UNCLASSIFIED	UNCLASSIFIED	UL

INTENTIONALLY LEFT BLANK.

USER EVALUATION SHEET/CHANGE OF ADDRESS

This Laboratory undertakes a continuing effort to improve the quality of the reports it publishes. Your comments/answers to the items/questions below will aid us in our efforts.

1. ARL Report Number/Author ARL-TR-1407 (Bar-On) Date of Report June 1997

2. Date Report Received _____

3. Does this report satisfy a need? (Comment on purpose, related project, or other area of interest for which the report will be used.) _____

4. Specifically, how is the report being used? (Information source, design data, procedure, source of ideas, etc.) _____

5. Has the information in this report led to any quantitative savings as far as man-hours or dollars saved, operating costs avoided, or efficiencies achieved, etc? If so, please elaborate. _____

6. General Comments. What do you think should be changed to improve future reports? (Indicate changes to organization, technical content, format, etc.) _____

CURRENT ADDRESS

_____
Organization

_____
Name E-mail Name

_____
Street or P.O. Box No.

_____
City, State, Zip Code

7. If indicating a Change of Address or Address Correction, please provide the Current or Correct address above and the Old or Incorrect address below.

OLD ADDRESS

_____
Organization

_____
Name

_____
Street or P.O. Box No.

_____
City, State, Zip Code

(Remove this sheet, fold as indicated, tape closed, and mail.)
(DO NOT STAPLE)

DEPARTMENT OF THE ARMY

OFFICIAL BUSINESS

NO POSTAGE
NECESSARY
IF MAILED
IN THE
UNITED STATES

BUSINESS REPLY MAIL
FIRST CLASS PERMIT NO 0001,APG,MD

POSTAGE WILL BE PAID BY ADDRESSEE

DIRECTOR
US ARMY RESEARCH LABORATORY
ATTN AMSRL WM MD
ABERDEEN PROVING GROUND MD 21005-5066